Laser & Optoelectronics Progress

One-Dimensional Modulational Instability of Broad Optical Beams In Photorefractive Crystals with Both Linear and Quadratic Electro-Optic Effects

Hao Lili[1], Wang Zhen[1], Tang Hongxia[2], Zhang Xiaoyang[1], Yang Qi[1], Wang Qiang[1*]

[1]*Department of Physics, College of physics and Electronic Engineering, Northeast Petroleum University, Daqing* 163318, *Heilongjiang, China*;

[2]*Department of Physics, College of Electrical Engineering, Suihua University, Suihua* 152000, *Heilongjiang, China*

Abstract We present a theoretical study of the one-dimensional modulational instability of a broad optical beam propagating in a biased photorefractive crystal with both linear and quadratic electro-optic effects (Kerr effect) under steady-state conditions. One-dimensional modulational instability growth rates are obtained by treating the space-charge field equation globally and locally. Both theoretical reasoning and numerical simulation show that both the global and local modulational instability gains are governed simultaneously by the strength and the polarity of external bias field and by the ratio of the intensity of the broad beam to that of the dark irradiance. Under a strong bias field, the results obtained using these two methods are in good agreement in the low spatial frequency regime. Moreover, the instability growth rate increases with the bias field, and the maximum instability growth occurs when ratio of light intensity to dark irradiance is 0. 88.

Key words nonlinear optics; photorefractive effects; spatial soliton; modulational instability

中图分类号 O437 **文献标志码** A **DOI:** 10.3788/LOP230900

1 Introduction

Photorefractive (PR) spatial solitons have been extensively investigated in the past two decades, in light of their unique features of formation on the order of a few mW and their important potential applications[1-4]. Various types of PR spatial solitons that arise from the change in refractive index due to only the linear electro-optic effect (Pockels effect) in noncentrosymmetric PR crystals or the quadratic electro-optic effect (DC Kerr effect) in centrosymmetric PR crystals have been investigated both theoretically and experimentally[5-8]. Moreover, under proper conditions, PR spatial solitons and soliton pairs (or soliton families) governed by both the linear and quadratic EO effects have been proven to exist in many noncentrosymmetric PR crystals when the crystal temperature is close to its phase-transition temperature[9-12].

Modulational instability (MI) refers to the interplay between nonlinearity and diffraction or dispersion in the spatial or temporal domain, which occur in most nonlinear optical wave systems[13-16]. For a plane wave or broad optical beam that propagates in a nonlinear optical medium, spatial MI causes the incident beam to disintegrate during propagation, which in turn leads to the formation of multiple wave filaments. The filaments resulting from the MI process can be considered as ideal soliton trains. In other words, solitons are tightly connected to the MI. Because MI typically occurs in the same parameter region in which bright solitons are observed, it is considered a precursor to soliton formation. To date, MI has been systematically

收稿日期：2023-03-20；**修回日期**：2023-04-06；**录用日期**：2023-04-20；**网络首发日期**：2023-04-29

基金项目：黑龙江省教育教学规划课题项目(GJB1320038, GJB1422173)、黑龙江省高校基础研究基金研究项目(KYYWF10236190106)、东北石油大学教育教学改革项目(JGXM_NEPU_202114)、东北石油大学主导创新基金项目(2021YDL-16)

通信作者：*wangqiang8035@163.com

investigated in biased photorefractive crystals owing to single- or two-photon photorefractive effect[17-20]. Previous studies of MI in the context of photorefractive processes have been limited to photorefractive materials, in which the change in the refractive index is governed solely by the linear or quadratic electro-optic effect. In fact, incident beams propagating in photorefractive media with both linear and quadratic electro-optic effects experience refractive index modulation, which can strongly influence MI.

In this paper, we present a theoretical study of the MI of broad beams in biased PR crystals with both linear and quadratic electro-optic effects by treating the space-charge field globally and locally, whereby both the one-dimensional global and local MI growth rates are obtained. The properties of these MI growth rates that differ from previous results are discussed, and relevant examples are provided.

2 Theoretical model

In order to investigate the modulational instability of a broad optical beam in biased PR crystals with both the linear and quadratic electro-optic effects, we consider a broad optical beam that propagates along the z-axis, where the PR crystal is placed with its principal axes aligned with the x, y and z directions of the system. The polarization of the broad beam and the external bias electric field are both assumed to be parallel to the x-axis. For simplicity, only x-axis diffraction will be considered, and any loss effects are neglected in our analysis.

The optical field of the incident beam is expressed as the slowly varying envelopes $\vec{E}(x,z)=\hat{x}\varphi(x,z)\exp(\mathrm{i}kz)$, where $k=k_0n_e=(2\pi/\lambda_0)n_e$ with n_e being the unperturbed index of refraction and λ_0 the free-space wavelength, and $\hat{x}$ is the unit vector along x. Under the above conditions, the optical beam[2,21] satisfies the following equation

$$\left(\mathrm{i}\frac{\partial}{\partial z}+\frac{1}{2k}\cdot\frac{\partial^2}{\partial x^2}+\frac{k}{n_e}\Delta n\right)\varphi(x,z)=0. \tag{1}$$

The change of nonlinear refractive index Δn is governed by

$$\Delta n=-\frac{n_e^3 r_{33}E_{sc}}{2}-\frac{n_e^3 g_{eff}\varepsilon_0^2(\varepsilon_r-1)^2E_{sc}^2}{2}, \tag{2}$$

where $\varphi(x,z)$ is the slowly varying envelope of the optical beam and r_{33} and g_{eff} are the linear and effective quadratic electro-optic coefficients of the PR crystal, respectively. Further, $k=k_0n_e=(2\pi/\lambda_0)n_e$ with n_e the unperturbed index of refraction and λ_0 the free-space wavelength, and ε_0 and ε_r denote vacuum and relative dielectric constants, respectively. By substituting Eq. (2) into Eq. (1), we obtain the following paraxial equation:

$$\mathrm{i}\frac{\partial U}{\partial z}+\frac{1}{2k}\frac{\partial^2 U}{\partial x^2}-\beta_1E_{sc}U-\beta_2E_{sc}^2U=0, \tag{3}$$

where $\beta_1=k_0n_e^3r_{33}/2$, $\beta_2=k_0n_e^3g_{eff}\varepsilon_0^2(\varepsilon_r-1)^2/2$, $U=\left(2\eta_0I_d/n_e\right)^{-1/2}\varphi(x,z)$, and the power density of the broad beam has been normalized to the so-called "dark-irradiance" I_d, i. e., $I=\left(n_e/2\eta_0\right)|\varphi|^2$ with $\eta_0=\left(\mu_0/\varepsilon_0\right)^{1/2}$. Based on the transport model of Kukhtarev et al., the space-charge field E_{sc}[3] in the material is approximately given by

$$E_{sc}=E_0\frac{1}{\left[1+|U|^2\right]}\left(1+\frac{\varepsilon_0\varepsilon_r}{eN_A}\cdot\frac{\partial E_{sc}}{\partial x}\right)-\frac{K_BT}{e}\frac{\left[\partial|U|^2/\partial x\right]}{\left[1+|U|^2\right]}+\frac{K_BT}{e}\cdot\frac{\varepsilon_0\varepsilon_r}{eN_A}\cdot\left(1+\frac{\varepsilon_0\varepsilon_r}{eN_A}\frac{\partial E_{sc}}{\partial x}\right)^{-1}\frac{\partial^2E_{sc}}{\partial x^2}. \tag{4}$$

For the bright type, $|U|^2=0$ at $x\to\pm\infty$, where E_0 represents the value of the space-charge field at $x\to\pm\infty$, i. e., $E_0=E_{sc}(x\to\pm\infty,z)$, e is the charge, K_B is Boltzmann's constant, T is the absolute temperature, and N_A is the acceptor or trap density. It is worth noting that the diffusion term $(2k)^{-1}(\partial^2U/\partial x^2)$ and the spatial derivatives of E_{sc} and U can be omitted in Eqs. (3) and (4), because U remains relatively constant over a large range of x for broad beams. Under the above conditions, the space-charge field E_{sc} is given by

$$E_{sc}=\frac{E_0}{1+|U|^2}. \tag{5}$$

We begin our analysis by treating the space-charge field equation in Eq. (4) globally. In this case,

$$U=r^{1/2}\exp\left\{-\mathrm{i}\left\{\left[\beta_1E_0/(1+r)\right]+\left[\beta_2E_0^2/(1+r)^2\right]\right\}z\right\}, \tag{6}$$

where r is defined as $r=I_{max}/I_d=I(0)/I_d$. In what follows, we discuss the stability of the above solution by making the following ansatz:

$$U=\left[r^{1/2}+\varepsilon(x,z)\right]\exp\left\{-\mathrm{i}\left\{\left[\beta_1E_0/(1+r)\right]+\left[\beta_2E_0^2/(1+r)^2\right]\right\}z\right\}, \tag{7}$$

here $\varepsilon(x,z)$ represents an added weak spatial perturbation term and satisfies the condition $|\varepsilon(x,z)| \ll r^{1/2}$. Substitution of Eq. (7) into Eqs. (3) and (4) yields:

$$\mathrm{i}\frac{\partial \varepsilon}{\partial z}+\frac{1}{2k}\frac{\partial^2 \varepsilon}{\partial x^2}-\left[\beta_1+\beta_2(E+2E_{01})\right](r^{1/2}+\varepsilon)E=0, \tag{8}$$

$$E-\upsilon\frac{\partial E}{\partial x}-\Delta\frac{\partial^2 E}{\partial x^2}=-\frac{r^{1/2}}{(1+r)}\left[E_{01}(\varepsilon+\varepsilon^*)+\frac{K_B T}{e}\left(\frac{\partial \varepsilon}{\partial x}+\frac{\partial \varepsilon^*}{\partial x}\right)\right], \tag{9}$$

where $E=E_{sc}-E_{01}$, $E_{01}=E_0/(1+r)$, $\upsilon=E_{01}(\varepsilon_0\varepsilon_r/eN_A)$, $\Delta=(K_B T/e)(\varepsilon_0\varepsilon_r/eN_A)$. The space-charge field in the spatial-frequency space $\hat{E}$ can then be obtained by employing the Fourier transform, satisfying

$$\hat{E}=-\frac{r^{1/2}}{(1+r)}\cdot\left\{\frac{E_{01}+\mathrm{i}\left[\upsilon E_{01}k_x+k_x(K_B T/e)(1+\Delta k_x^2)\right]}{(1+\Delta k_x^2)^2+k_x^2\upsilon^2}\right\}\cdot(\hat{\varepsilon}+\hat{\varepsilon}^*), \tag{10}$$

where $\hat{\varepsilon}$ is the Fourier transform of the spatial perturbation in the spatial-frequency space. The spatial perturbation $\varepsilon(x,z)$ can be expressed as the sum of the following two terms:

$$\varepsilon=a(z)\exp(\mathrm{i}px)+b(z)\exp(-\mathrm{i}px). \tag{11}$$

It is easy to show that

$$(\hat{\varepsilon}+\hat{\varepsilon}^*)=2\pi\left[(a+b^*)\delta(k_x-p)+(b+a^*)\cdot\delta(k_x+p)\right], \tag{12}$$

where $\delta(k_x)$ is the delta function. Substituting this form of $(\hat{\varepsilon}+\hat{\varepsilon}^*)$ back into Eq. (10) and taking an inverse Fourier transform allows the space-charge field in real space to be obtained from the following equation:

$$E=-\frac{r^{1/2}}{1+r}(a+b^*)\cdot\frac{E_{01}+\mathrm{i}\left[\upsilon E_{01}p+p(K_B T/e)(1+\Delta p^2)\right]}{(1+\Delta p^2)^2+p^2\upsilon^2}\exp(\mathrm{i}px)-\frac{r^{1/2}}{1+r}(a^*+b)\frac{E_{01}-\mathrm{i}\left[\upsilon E_{01}p+p(K_B T/e)(1+\Delta p^2)\right]}{(1+\Delta p^2)^2+p^2\upsilon^2}\cdot\exp(-\mathrm{i}px). \tag{13}$$

In order to simplify calculations, $G(p)$ is defined as

$$G(p)=\frac{r}{1+r}\frac{E_{01}+\mathrm{i}\left[\upsilon E_{01}p+p(K_B T/e)(1+\Delta p^2)\right]}{(1+\Delta p^2)^2+p^2\upsilon^2}. \tag{14}$$

Eq. (13) then reduces to

$$E=-r^{-1/2}\left[G(p)(a+b^*)\exp(\mathrm{i}px)+G^*(p)(a^*+b)\exp(-\mathrm{i}px)\right]. \tag{15}$$

By substituting Eqs. (11) and (13) into Eq. (8) and keeping only the synchronous terms, we obtain to the following coupled differential equations:

$$\mathrm{i}\frac{\mathrm{d}a}{\mathrm{d}z}-\frac{p^2}{2k}a+(\beta_1+2\beta_2E_{01})G(p)(a+b^*)=0, \tag{16a}$$

$$\mathrm{i}\frac{\mathrm{d}b}{\mathrm{d}z}-\frac{p^2}{2k}b+(\beta_1+2\beta_2E_{01})G^*(p)(a^*+b)=0. \tag{16b}$$

We then decouple Eqs. (16) into an equivalent set of ordinary differential equations as follows:

$$\frac{\mathrm{d}^2 a}{\mathrm{d}z^2}=\left[\frac{p^2}{k}(\beta_1+2\beta_2E_{01})G(p)-\frac{p^4}{4k^2}\right]a, \tag{17a}$$

$$\frac{\mathrm{d}^2 b}{\mathrm{d}z^2}=\left[\frac{p^2}{k}(\beta_1+2\beta_2E_{01})G^*(p)-\frac{p^4}{4k^2}\right]b. \tag{17b}$$

From these two equations, we can directly obtain the global modulational instability gain g_{gl} as

$$g_{gl}=\mathrm{Re}\left\{\left[\frac{p^2}{k}(\beta_1+2\beta_2E_{01})G(p)-\frac{p^4}{4k^2}\right]^{1/2}\right\}, \tag{18}$$

where $\mathrm{Re}\{\cdot\}$ denotes the real part of a complex variable. From Eq. (13), it is clear that the MI gain is an even function of p, and that its value reaches zero at $p=0$.

The local MI process deserves special consideration. In the next section, the local MI process is investigated theoretically by neglecting higher-order effects in the space-charge field. Under strong bias conditions, for a broad incident optical beam the diffusion effect can be neglected; that is, all terms associated with the diffusion process (i. e., $K_B T$ terms) may be omitted in Eq. (4). Additionally, the dimensionless term $(\varepsilon_0\varepsilon_r/eN_A)(\partial E_{sc}/\partial x)$ is typically significantly less than unity[17]. Accordingly, the paraxial Eq. (3) reduces to

$$\mathrm{i}\frac{\partial U}{\partial z}+\frac{1}{2k}\frac{\partial^2 U}{\partial x^2}-\beta_1 E_0\frac{U}{1+|U|^2}-\beta_2 E_0^2\frac{U}{(1+|U|^2)^2}=0, \tag{19}$$

Eq. (19) takes the form of a nonlinear Schrödinger equation with a saturable nonlinearity. In our preliminary work, we obtained the solitary wave solutions of dark, bright, and grey solitons in a steady-state regime, various of whose characteristics and properties have been discussed in detail elsewhere[9-10]. In what follows, by introducing Eq. (7) into Eq. (19) and linearizing it in ε, the local MI properties of Eq. (19) can be investigated using the following evolution equation.

$$\mathrm{i}\frac{\partial \varepsilon}{\partial z}+\frac{1}{2k}\frac{\partial^2 \varepsilon}{\partial x^2}+\beta_1 E_0\frac{r}{(1+r)^2}(\varepsilon+\varepsilon^*)+2\beta_2 E_0^2\frac{r}{(1+r)^3}(\varepsilon+\varepsilon^*)=0. \tag{20}$$

Substituting Eq. (11) into Eq. (20), we obtain

$$\mathrm{i}\frac{\mathrm{d}a}{\mathrm{d}z}-\frac{p^2}{2k}a+\beta_1 E_0\frac{r}{(1+r)^2}(a+b^*)+2\beta_2 E_0^2\frac{r}{(1+r)^3}(a+b^*)=0, \tag{21a}$$

$$\mathrm{i}\frac{\mathrm{d}b}{\mathrm{d}z}-\frac{p^2}{2k}b+\beta_1 E_0\frac{r}{(1+r)^2}(a^*+b)+2\beta_2 E_0^2\frac{r}{(1+r)^3}(a^*+b)=0. \tag{21b}$$

The above equations can be decoupled into an equivalent set of ordinary differential equations:

$$\frac{\mathrm{d}^2 a}{\mathrm{d}z^2}=\left\{-\frac{p^4}{4k^2}+\left[\beta_1 E_0\frac{r}{(1+r)^2}+2\beta_2 E_0^2\frac{r}{(1+r)^3}\right]\frac{p^2}{k}\right\}a, \tag{22a}$$

$$\frac{\mathrm{d}^2 b}{\mathrm{d}z^2}=\left\{-\frac{p^4}{4k^2}+\left[\beta_1 E_0\frac{r}{(1+r)^2}+2\beta_2 E_0^2\frac{r}{(1+r)^3}\right]\frac{p^2}{k}\right\}b, \tag{22b}$$

and the local MI gain can be obtained directly from Eq. (23):

$$g_{\mathrm{lc}}=\mathrm{Re}\left\{\left[-\frac{p^4}{4k^2}+\left(\beta_1 E_0\frac{r}{(1+r)^2}+2\beta_2 E_0^2\frac{r}{(1+r)^3}\right)\frac{p^2}{k}\right]^{1/2}\right\}. \tag{23}$$

Moreover, the maximum MI gain and its associated spatial frequency can be readily determined as follows:

$$g_{\max}=\frac{k_0 n_e^3 r_{33} E_0}{2}\frac{r}{(1+r)^2}+k_0 n_e^3 g_{\mathrm{eff}}\varepsilon_0^2(\varepsilon_r-1)^2 E_0^2\frac{r}{(1+r)^3}, \tag{24}$$

$$p_{\max}=\frac{k_0 n_e^2}{1+r}\left\{E_0 r\left[r_{33}+\frac{2g_{\mathrm{eff}}\varepsilon_0^2(\varepsilon_r-1)^2 E_0}{1+r}\right]\right\}^{1/2}. \tag{25}$$

3 Results and discussions

To illustrate our results, we consider a single PMN-0.33PT crystal that exhibits maximal transparency, very good optical clarity, and low propagation loss. The parameters of PMN-0.33PT are $n_e=2.562$, $r_{33}=182\ \mathrm{pm/V}$, $g_{\mathrm{eff}}=0.06\ \mathrm{m^4\cdot C^{-2}}$, $\varepsilon_r=5378$, $N_A=3.7\times10^{22}\ \mathrm{m^{-3}}$[22-25]. The other parameters are set as $\lambda_0=632.8\ \mathrm{nm}$ and $x_0=40\ \mu\mathrm{m}$. Based on these parameters, $\beta_1=0.0152$, $\beta_2=1.1354\times10^{-8}$, and $k=2.5439\times10^7$.

Figs. 1 and 2 show the dependence of the global and local MI gains (i. e., g_{gl} and g_{lc}) on p/k with three different values of E_0 for the same r, where the dimensionless ratio p/k represents the angle (in radians) at which the plane-wave components of the $\varepsilon(x,z)$ perturbation propagate with respect to the quasi-plane-wave optical beam. From these two figures, it is evident that the two MI gains increase with increasing E_0. Given that both gains are symmetrical about p, only the positive branch will be considered in our subsequent analyses. From Fig. 1, we can observe that the global MI gain curve reaches two different peaks: one appears in the low spatial-frequency domain, defined as g_{p1}, and the other occurs in the high-frequency region, defined as g_{p2}. Moreover, it is evident that both E_0 and r affect these two different peaks. Next, we study the effects of E_0 and r in isolation on MI gains using a variable-controlling approach.

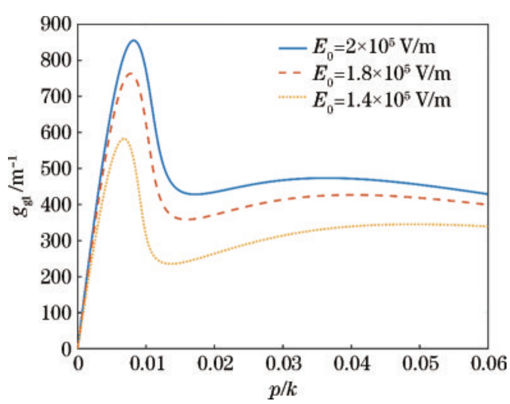

Fig. 1 Global MI gains as a function of p/k when $r=1$

We begin with the effect arising from the biased field E_0. Fig. 3 depicts the curve of the global MI gains versus E_0 associated with the two global peaks p_1/k and

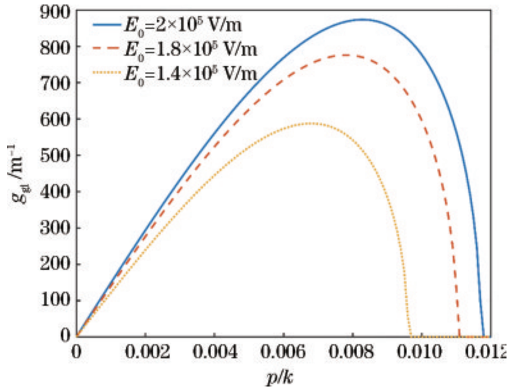

Fig. 2 Local MI gains as a function of p/k when $r=1$

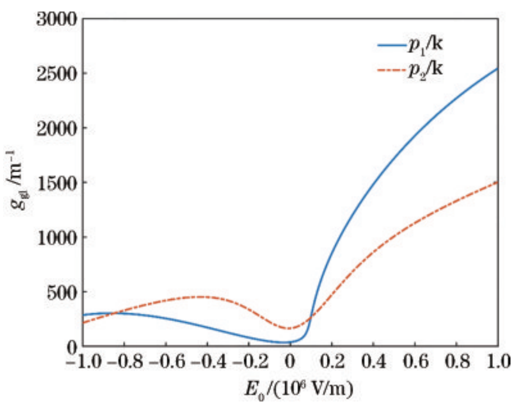

Fig. 3 Dependence of the global MI gains associated with the two global spatial-frequencies peaks p_1/k and p_2/k on E_0 when $r=1$

p_2/k. Unlike the cases investigated previously, we find that the global MI gains are asymmetric with respect to the polarity of E_0, that is, the global MI gains depend not only on the absolute strength of E_0, but also on the polarity of the external bias electric field E_0. This is because the global MI gains are governed by both linear and quadratic electrooptic effects. By altering the polarity of E_0, the sign of the linear electro-optic term $\left(\beta_1 E_0 \propto E_0\right)$ changes as well. However, the sign of the quadratic electro-optic term $\left(\beta_2 E_0^2 \propto E_0^2\right)$ is not influenced by the polarity change of E_0, so in the case of an externally biased field of equal magnitude but opposite polarity, the photorefractive effect is weakened and even counteracted by the interaction between the linear and quadratic electric-optic effects. Global MI gains can also be adjusted by altering the polarity of E_0 in addition to changing its strength. Furthermore, Fig. 3 shows that g_{p1} exceeds g_{p2} when $E_0 > 1\times 10^5$ V/m with the positive bias field.

In addition, Fig. 4 illustrates the dependence of the global MI gain peak g_{p1} and g_{p2} on r for $E_0=1.8\times 10^5$ V/m. As shown in Fig. 3, g_{p1} and g_{p2} attain their maxima at $r\approx 1$. Moreover, the peak g_{p1} decreases rapidly when $r \ll 0.1$ and $r \gg 10$, and all g_{p1} and g_{p2} tend to be stable for $r \gg 10$.

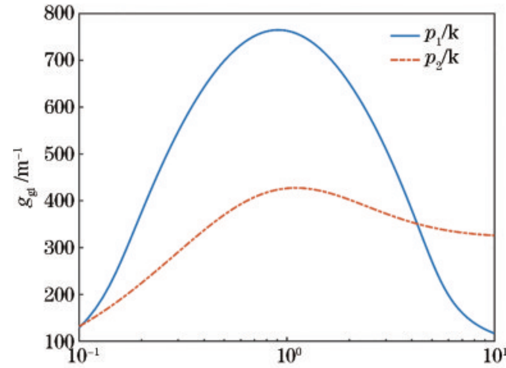

Fig. 4 Dependence of the global MI gains associated with the two global peak spatial-frequencies p_1/k and p_2/k on r when $E_0=1.8\times 10^5$ V/m

Fig. 5 shows the variation of the two gain peaks g_{p1} and g_{p2} as a function of both E_0 and p/k when $r=1$, from which we can see that in the low bias voltage region $g_{p1} < g_{p2}$, and g_{p1} will exceed g_{p2} when E_0 is higher than a certain value. Moreover, in the low spatial-frequency domain g_{p1} tends to increase linearly with increasing E_0; however, g_{p2} increases slowly in the high spatial-frequency domain under different p/k conditions. In fact, under strong bias conditions the MI process should be treated with the local process and Eqs. (16) can be simplified to Eq. (21).

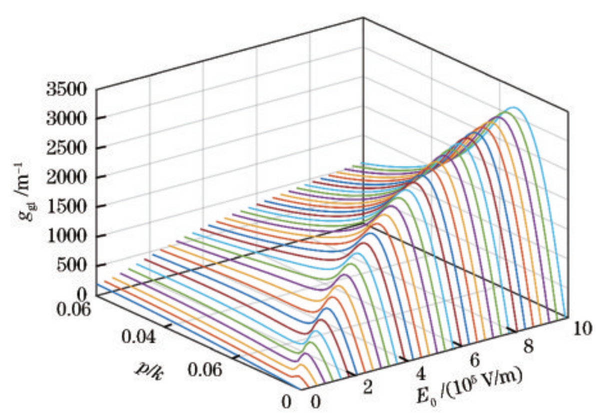

Fig. 5 Dynamical evolution of the global g_{p1} and g_{p2} versus both E_0 and p/k when $r=1$

Fig. 6 shows the dependence of the global gains g_{gl} on p/k with different r in the case of $E_0=1.8\times 10^5$ V/m. The maximum value of g_{gl} (i. e., g_{max}) appears in the low-spatial-frequency domain when r is small; however, g_{max} arises in the high-spatial-frequency regime when r is relatively large.

In contrast to the results obtained previously, we find that both g_{max} and p_{max} follow the quadratic

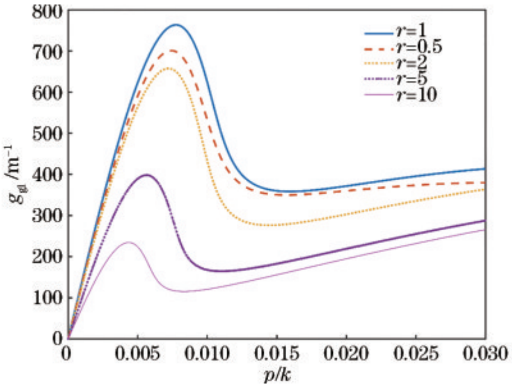

Fig. 6　The global MI gains as a function of p/k under different r conditions for $E_0 = 1.8 \times 10^5$ V/m

polynomials of E_0, and the maximum MI gains increase rapidly with an increase in the external bias field according to Eqs. (24) and (25), respectively. In addition, the MI gain can be adjusted by altering the polarity of the external bias field, even for the same bias field strength. Moreover, further analysis of Eqs. (24) and (25) shows that g_{max} and p_{max} reach a maximum when $r = 0.88$.

4　Conclusions

We investigated the one-dimensional modulational instability of a broad optical beam propagating in biased PR crystals with both linear and quadratic electro-optic effects under steady-state conditions. Both the one-dimensional global and local MI growth rates were obtained by treating the space-charge field equation globally and locally. It was shown that the global and local modulational instability gains were governed simultaneously by the strength and polarity of the external bias field and the ratio of the intensity of the broad beam to that of the dark irradiance. This means that the spatial period of spontaneously generated filaments can be controlled by adjusting the factors mentioned above. Moreover, under a strong bias field, the results obtained from these two methods were in good agreement in the low spatial frequency regime. The instability growth rates increase with the bias field, and the maximum instability growth occurs at $r = 0.88$.

References

[1] Delre E, Crosignani B, Tamburrini M, et al. One-dimensional steady-state photorefractive spatial solitons in centrosymmetric paraelectric potassium lithium tantalate niobate[J]. Optics letters, 1998, 23(6): 421-423.

[2] Liu C H, Cao Y Q, Tang X H, et al. Research status and progress of dissipative soliton resonance pulsed fiber lasers[J]. Chinese Journal of Lasers, 2022, 49(21): 2100002.

[3] Zhou Y C, Qin Z P, Xie G Q. 2.8 μm Er:ZBLAN fiber soliton self-compression amplifier[J]. Chinese Journal of Lasers, 2022, 49(1): 0101009.

[4] Tong H, Wang F Y, Qin Z P, et al. Temporal-filtering dissipative soliton in an optical parametric oscillator[J]. High Power Laser Science and Engineering, 2022, 10(2): e16.

[5] Duree G, Shultz J, Salamo G J, et al. Observation of self-trapping of an optical beam due to the photorefractive effect[J]. Physical review letters, 1993, 71(4): 533-536.

[6] Cohen O, Carmon T, Segev M, et al. Holographic solitons[J]. Optics Letters, 2002, 27(22): 2031-2033.

[7] Xu Y, Liang W, Yariv A, et al. High-quality-factor Bragg onion resonators with omnidirectional reflector cladding[J]. Optics Letters, 2003, 28(22): 2144-2146.

[8] Wu J, Li Q L, Zhang Z Z, et al. Low half-wave voltage lithium niobate electro-optic slitter based on dual crystal matching[J]. Chinese Journal of Lasers, 2022, 49(7): 0708001.

[9] Hao L L, Wang Q A, Hou C F. Spatial solitons in biased photorefractive materials with both the linear and quadratic electro-optic effects[J]. Journal of Modern Optics, 2014, 61(15): 1236-1245.

[10] Hao L L, Hou C F, Wang Q. Spatial solitons in biased two-photon photorefractive crystals with both the linear and quadratic electro-optic effect[J]. Optics & Laser Technology, 2014, 56: 326-333.

[11] Jiang Q C, Su Y L, Nie H X, et al. Separate spatial soliton pairs in a biased series photorefractive crystal circuit with both the linear and quadratic electro-optic effects[J]. Journal of Modern Optics, 2017, 64(6): 609-615.

[12] Katti A, Katti C P. Gap solitons supported by an optical lattice in biased photorefractive crystals having both the linear and quadratic electro-optic effect[J]. Zeitschrift Für Naturforschung A, 2020, 75(9): 749-756.

[13] Soljacic M, Segev M, Coskun T, et al. Modulation instability of incoherent beams in noninstantaneous nonlinear media[J]. Physical Review Letters, 2000, 84(3): 467-470.

[14] Kivshar Y S, Peyrard M. Modulational instabilities in discrete lattices[J]. Physical Review A, 1992, 46(6): 3198-3205.

[15] Kip D, Soljačić M, Segev M, et al. (1+1)-Dimensional modulation instability of spatially incoherent light[J]. Journal of the Optical Society of America B, 2002, 19(3): 502-512.

[16] Miller P D, Bang O. Macroscopic dynamics in quadratic nonlinear lattices[J]. Physical Review E, 1998, 57(5): 6038-6049.

[17] Carvalho M I, Singh S R, Christodoulides D N. Self-deflection of steady-state bright spatial solitons in biased photorefractive crystals[J]. Optics Communications, 1995, 120(5/6): 311-315.

[18] Pu S Z, Hou C F, Zhan K Y, et al. Beam splitters in inhomogeneous nonlocal media[J]. Physica Scripta,

2012, 86(2): 025404.

[19] Lu K Q, Zhao W, Yang Y L, et al. Waveguides induced by steady-state gray solitons in biased photorefractive-photovoltaic crystals[J]. Optics Communications, 2008, 281(1): 49-54.

[20] Katti A, Yadav R A. Modulation instability of broad optical beams in unbiased photorefractive pyroelectric crystals[J]. Chaos, Solitons & Fractals, 2017, 101: 20-23.

[21] Akhouri B P, Gupta P K. Potential formalism of optical spatial soliton propagation in a two-photon photovoltaic-photorefractive material under open circuit condition[J]. Indian Journal of Physics, 2014, 88(4): 421-425.

[22] Wan X M, Wang D Y, Zhao X Y, et al. Electro-optic characterization of tetragonal $(1-x)Pb(Mg_{1/3}Nb_{2/3})O_3$-$xPbTiO_3$ single crystals by a modified Sénarmont setup [J]. Solid State Communications, 2005, 134(8): 547-551.

[23] Kumar P, Sharma S, Thakur O P, et al. Dielectric, piezoelectric and pyroelectric properties of PMN-PT (68: 32) system[J]. Ceramics International, 2004, 30(4): 585-589.

[24] Zhang R, Jiang B, Cao W W. Single-domain properties of $0.67Pb(Mg_{1/3}Nb_{2/3})O_3$-$0.33PbTiO_3$ single crystals under electric field bias[J]. Applied Physics Letters, 2003, 82 (5): 787-789.

[25] Wei Z H, Huang Y L, Tsuboi T, et al. Optical characteristics of Er^{3+}-doped PMN-PT transparent ceramics[J]. Ceramics International, 2012, 38(4): 3397-3402.